IEEE ANTENNAS AND WIRELESS PROPAGATION LETTERS, vol. 17, no. 8, pp. 1421-1425, Aug. 2018, DOI: 10.1109/LAWP.2018.2848719

Bifocal Design Procedure for Dual Reflectarray Antennas in Offset Configurations

Eduardo Martinez-de-Rioja, Jose A. Encinar, Antonio Pino, Borja Gonzalez-Valdes, Sean V. Hum, and Carolina Tienda

Abstract—**This paper presents a new bifocal design procedure for dual reflectarray antennas in offset configurations. The technique starts by considering an axially symmetric geometry with the reflectarrays placed in parallel planes, which allows the rotation of a 2D bifocal design around the symmetry axis. To reach a more compact configuration and obtain smoother phase distributions, the reflectarrays are tilted and their phases adjusted by means of a ray-tracing routine. The technique has been validated by numerical simulations through the comparison with a previous center-fed dual reflectarray prototype. Finally, the simulations of an offset dual reflectarray antenna with tilted reflectarrays are presented, providing 0.56º beam spacing at 20 GHz for multi-spot satellite applications in Ka-band.**

Index Terms—**Bifocal technique, dual reflectarray antennas, multiple beam antennas, communication satellites.**

I. Introduction

THE BIFOCAL technique has been used to obtain an improved multiple beam and beam scanning performance of dual reflector systems with respect to conventional single-focus antennas [1]-[7]. The simplest approach for the design of bifocal dual reflectors exploits the use of axially symmetric geometries, which allow the rotation of a 2D bifocal design around the antenna symmetry axis [1]. Centered and offset configurations can be obtained by this procedure [2]-[4].

A dual reflectarray antenna (DRAA) provides control of the phase in two reflective surfaces, which can be used to improve the antenna performance with respect to single reflectarrays [8]-[11]. The bifocal technique has been applied to center-fed DRAAs, keeping a similar approach based on rotationally symmetric geometries [12]-[13]. A small-size centered DRAA (named the folded reflectarray antenna) was proposed in [12] for providing an enhanced field of view in automotive radars. The limitation of the folded configuration is that the antenna can only operate in single linear-polarization, since blockage from the sub-reflectarray is avoided by a gridded sub-reflector and a 90º twist of polarization on the main reflectarray.

The use of an offset DRAA configuration would allow to minimize sub-reflector blockage at the same time as enabling dual polarization operation of the bifocal antenna. This feature can be attractive for multi-beam antennas for current multi-spot satellite applications in Ka-band, based on frequency and polarization reuse [14]-[17]. However, the lack of symmetry of the offset DRAA configurations, where there is a relative tilt between the two reflectarrays, increases the complexity of the 3D design process. The problem of the bifocal technique applied to offset DRAAs was first addressed in [18], where Rappaport's technique [5] was used to shape the surfaces of an offset dual reflector configuration, and then, the phases on the equivalent reflectarrays that should emulate the reflectors were obtained from the distances between the reflectarray plane and the corresponding reflector. This approach implies several approximations and the results were not satisfactory.

In this paper, the authors propose a new bifocal design procedure applied directly to dual reflectarrays in offset configurations. The technique starts by considering an axially symmetric geometry with the reflectarrays placed in parallel planes. An offset DRAA configuration is formed after rotating a 2D bifocal design around the symmetry axis. Finally, both reflectarrays are tilted to obtain smoother phase distributions by means of a ray-tracing routine applied in the offset plane.

II. Bifocal Design Method for Dual Reflectarray Antennas in Offset Configurations

The geometric parameters that define an axially symmetric DRAA configuration with parallel reflectarrays (shown in Fig. 1) are: distance between foci (d), distance between the foci and the sub-reflectarray (L_1), distance between the two reflectarrays (L_2), and beam directions associated to the foci (θ_{b1} and θ_{b2}). The focal points (F_1 and F_2) are symmetric with respect to z-axis, and the same applies for θ_{b1} and θ_{b2}, which fulfill $\theta_{b1} = -\theta_{b2}$ (being $\theta_{b1} > 0º$ in the case shown in Fig. 1).

The first step of the proposed bifocal method consists on an iterative 2D ray-tracing routine applied in the xz-plane. The value of the phase derivative with respect to x (Φ'_x) will be determined for a discrete set of points on the vertical axis of each reflectarray in the xz-plane [19]. The first iteration of the ray-tracing routine starts with a transmitted ray from F_1 that impinges on the sub-reflectarray at point $S_1 = (0, 0, L_2)$ located on the symmetry axis of the DRAA system, so that its phase

This work was supported by the Spanish Ministry of Economy under Project TEC2016-75103-C2-1-R, and by the European Space Agency ESTEC under Contract 4000117113/16/NL/AF.

E. Martinez-de-Rioja and J. A. Encinar are with the Information Processing and Telecomm. Center, Universidad Politécnica de Madrid, 28040 Madrid, Spain (e-mail: em.martinezderioja@upm.es; jose.encinar@upm.es).

A. Pino and B. Gonzalez-Valdes are with the Signal Theory and Communications Department, Universidade de Vigo, 36310 Vigo, Spain (e-mail: agpino@com.uvigo.es; bgvaldes@com.uvigo.es).

S. V. Hum is with the Electrical & Computer Engineering Dpt., University of Toronto, M5S 1A1 Toronto, ON, Canada (e-mail: sean.hum@utoronto.ca).

C. Tienda is with the Antenna Group, Airbus Defence & Space, SG1 2AS Stevenage, United Kingdom (e-mail: carolina.tienda-herrero@airbus.com).

derivative is $\Phi'_x(S_1) = 0$. The angle of the reflected ray (θ_{ref}) can be obtained from the incidence angle (θ_{inc}) and the phase derivative at S_1 by the following expression [12]:

$$\Phi'_x = \frac{\partial \Phi}{\partial x} = \frac{2\pi}{\lambda}\left(\sin\theta_{inc} - \sin\theta_{ref}\right) \quad (1)$$

The ray will impinge on the main reflectarray at point M_1 and will be reflected at an angle θ_{b1}. The value of $\Phi'_x(M_1)$ can be obtained by applying (1) again, since both the incidence and reflection angles are known. Then, a received ray in the direction θ_{b2} that impinges on M_1 will provide a new point on the sub-reflectarray, S_2, and the value of its phase derivative, $\Phi'_x(S_2)$, by enforcing the ray to reach focus F_2, following the same procedure as before. The next iteration of the ray tracing will start with a transmitted ray from F_1 that impinges on S_2. After N iterations, two sets of points are created in the *xz*-plane (S_i and M_i), one for each reflectarray. A polynomial interpolation of the Φ'_x samples provides the phase derivative curves required on each reflectarray, which are integrated to obtain the bifocal phases in the *xz*-plane, $\Phi_S(x)$ and $\Phi_M(x)$.

In order to improve the accuracy in the interpolation of the Φ'_x samples, the number of points that define each reflectarray can be doubled by a second execution of the ray-tracing routine starting at M_1'= (0, 0, 0) on the main reflectarray, also with $\Phi'_x(M_1) = 0$. A received ray in the direction θ_{b2} that impinges on M_1' provides a new point on the sub-reflectarray, S_1', and its phase derivative, $\Phi'_x(S_1')$, by applying (1) on both reflectarrays and enforcing the ray to reach focus F_2. Then, a transmitted ray from F_1 that impinges on S_1' can be used to continue with the previously described ray-tracing procedure.

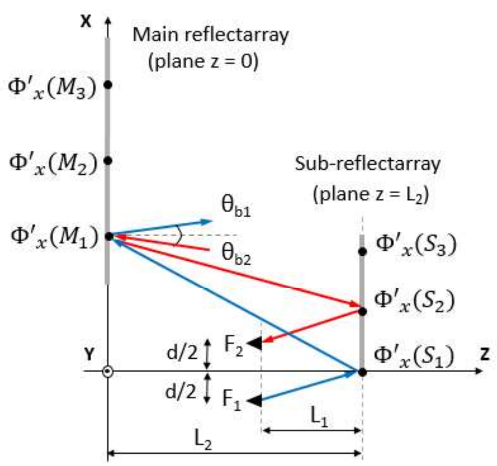

Fig. 1 Geometry of the dual reflectarray antenna (DRAA) and performance of the first iteration of the ray-tracing routine in the *xz*-plane.

The bifocal phase functions obtained in the *xz*-plane are rotated around the *z*-axis, so that a planar phase distribution is achieved for each reflectarray. These phases enable the design of both centered and offset DRAA configurations, simply by choosing specific portions of the planes $z = 0$ and $z = L_2$. In the case of offset configurations, the design with the reflectarrays placed in parallel planes results in fast variations in the phase-shift distributions of both reflectarrays (as will be shown in Section IV). To achieve a smoother phase variation, both the sub- and the main reflectarrays are tilted about their geometric centers by an angle θ_S and θ_M, respectively, as shown in Fig. 2. The foci are rotated along with the sub-reflectarray to maintain the same angles of incidence. The beam directions with respect to *z*-axis are the same than in the initial configuration, θ_{b1} and θ_{b2}, but the relative directions with respect to the normal vector to the main reflectarray surface ($\hat{z}_M$) are now $\theta_M + \theta_{b1}$ and $\theta_M + \theta_{b2}$. The values of θ_S and θ_M that provide the smoothest variation in the phase distributions can be estimated from the bifocal phase curves in the *xz*-plane (Φ_S and Φ_M) as:

$$\theta_S \approx \sin^{-1}\left[\frac{\max(\Delta\Phi_S)\cdot\lambda/2\pi}{D_S/2}\right] \quad (2)$$

$$\theta_M \approx 0.5\cdot\sin^{-1}\left[\frac{\max(\Delta\Phi_M)\cdot\lambda/2\pi}{D_M/2}\right] \quad (3)$$

where D_S and D_M are the diameters of each reflectarray, and $\max(\Delta\Phi_S)$ and $\max(\Delta\Phi_M)$ are the maximum variations of the unwrapped bifocal phases along each reflectarray in the *xz*-plane with respect to the central element. The 0.5 multiplying factor in the estimation of θ_M is due to the decision to keep the original beam directions in the absolute reference system, which compensates for half of the required inclination for the main reflectarray.

A phase adjustment technique has been implemented in order to compensate the effect of tilting the reflectarrays, preserving the bifocal characteristic of the phase distributions obtained by rotation. The technique is based on a 2D ray-tracing procedure applied in the *xz*-plane, which provides two sets of points along the vertical axes of both reflectarrays, together with the required phase adjustment that enforces the same beam directions as in the original configuration. The procedure starts with a transmitted ray from F_1 that impinges first on the sub-reflectarray at point S_1, and then on the main reflectarray at point M_1, as shown in Fig. 2(a). After tilting both reflectarrays, the ray has to be enforced to reach the same point M_1 on the main reflectarray (note that S_1 will remain the same, as the foci are rotated along with the sub-reflectarray), and then, the ray will be reflected with an angle $\theta_M + \theta_{b1}$ with respect to $\hat{z}_M$ (instead of θ_{b1}). Hence, there will be a variation in the path length from S_1 to the scanned aperture plane with respect to the initial configuration with parallel reflectarrays. Let $\Delta PL_{1,1}$ be the computed path length variation associated to the ray that impinges first on S_1 and then on M_1. The phase adjustments $\Delta\Phi(S_1)$ and $\Delta\Phi(M_1)$ that must be added to the phases introduced by the reflectarray cells must fulfill:

$$\frac{2\pi}{\lambda}\cdot\Delta PL_{1,1} = \Delta\Phi(S_1) + \Delta\Phi(M_1) \quad (4)$$

It is required to set an initial value for the phase adjustment associated with S_1, e. g., $\Delta\Phi(S_1) = \Delta\Phi_0$. The other constant, $\Delta\Phi(M_1)$, can be obtained by applying (4). Similarly, a received ray in the direction θ_{b2} that impinges first on the main reflectarray at M_1 and then on the sub-reflectarray at S_2 (as shown in Fig. 2(b)) is used to obtain the value of the phase adjustment associated with S_2. In this case, the path length variation will be $\Delta PL_{2,1}$, so $\Delta\Phi(S_2) = (2\pi/\lambda)\cdot\Delta PL_{2,1} - \Delta\Phi(M_1)$. The same process can be repeated starting with a transmitted ray from F_1 that impinges on S_2 and then on M_2. After several iterations, the samples of $\Delta\Phi(S_i)$ and $\Delta\Phi(M_i)$ are interpolated by polynomials to obtain the required phase adjustment on each reflectarray in the *xz*-plane. These phases will be added to the planar phase distributions obtained by rotation, so that the same phase adjustment will be applied to all the reflectarray cells in the same row (same *x* coordinate). The tilted DRAA with the adjusted phase distributions will exhibit the same bifocal characteristic of the original design in the *xz*-plane (as will be shown in Section IV), while presenting good results for the patterns in the orthogonal plane due to the effect of previous rotation of the phase curves around the *z*-axis.

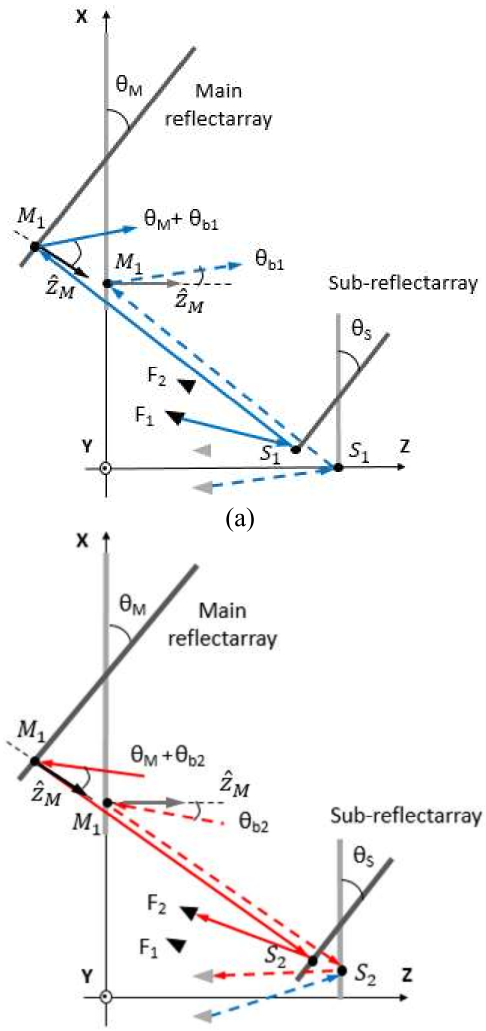

Fig. 2 Performance of the ray-tracing procedure used to compensate the tilt of both reflectarrays: (a) transmitted ray from F_1 and (b) received ray at F_2.

III. Validation for a Multi-beam DRAA in Folded Symmetrical Configuration

The proposed bifocal technique has been applied to design a center-fed DRAA for automotive radars at 76.5 GHz with the same configuration as the folded reflectarray prototype reported in [12] by other authors. The initial parameters of the DRAA system are: d = 1.6 cm, $L_1 = L_2$ = 2.6 cm, θ_{b1} = 9º and θ_{b2} = -9º. The bifocal phase curves required for each reflectarray in the *xz*-plane, as well as the position of the samples obtained after the ray tracing, are shown in Fig. 3. These phase curves have been rotated around the *z*-axis, and then, a centered configuration has been formed, resulting in two reflectarrays with diameters of 90 mm (derived from the ray tracing). A cell period of 2 mm (λ/2 at 75 GHz) has been considered. The DRAA has been simulated using the same analysis technique validated in previous works [8]-[9], and assuming ideal reflectarray cells that provide the required phase-shift at 76.5 GHz. In a practical implementation, the phase distributions will be realized using suitable reflectarray cells [20]-[21]. The selection of the reflectarray cells can be done so that a large bandwidth and reduced losses are obtained for the DRAA. For example, a 20% bandwidth in Ku-band (12-15 GHz) was achieved in [9] for a DRAA demonstrator designed with two layers of stacked rectangular patches. Bandwidth will be reduced for a large DRAA (as the case of section IV), but a 10% bandwidth is achievable.

The superposition of the simulated radiation patterns at 76.5 GHz for the designed DRAA and the measurements of the prototype presented in [12] is shown in Fig. 4, considering illumination from seven 3-mm diameter feed-horns with 4 mm separation (center to center), simulated by a $\cos^q(\theta)$ function with q = 3. A good agreement can be observed between both bifocal antennas, which validates the proposed implementation of the technique. The aperture efficiency of the designed DRAA at 76.5 GHz is around 67%. Moreover, an equivalent single-focus antenna with the same aperture size and F/D ratio has been designed, and the simulated radiation patterns for the central and the extreme beams have been included in Fig. 4. The scan loss in the monofocal antenna is 2.52 dB for ±13.5º beam angle, while in the bifocal antenna it is only 0.54 dB. The bifocal folded reflectarray can be suitable for those applications that require large scanning angles, though the need to eliminate blockage from the sub-reflectarray prevents the antenna from achieving dual-polarization capability [12]. The use of a centered DRAA configuration is imposed by the performance of the bifocal technique, which results in similar sizes for both reflectarrays, as can be inferred from the sample distributions obtained after the ray tracing, given in Fig. 3.

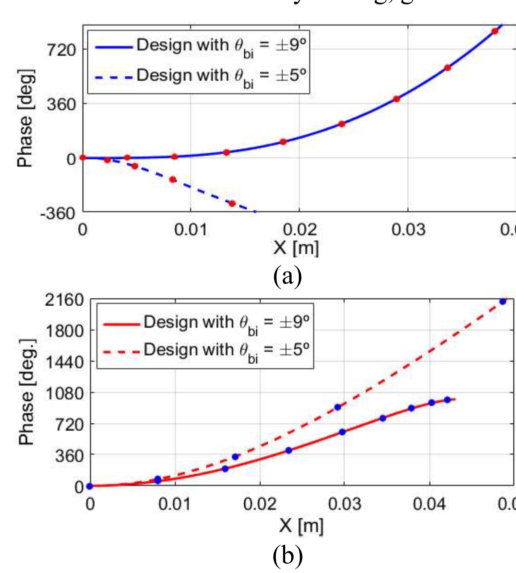

Fig. 3 Comparison of the phase curves and sample points obtained for two bifocal designs for (a) the sub-reflectarray and (b) the main reflectarray.

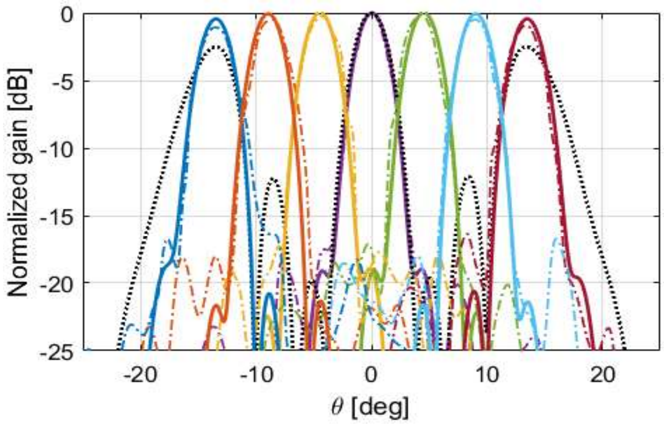

Fig. 4 Simulated radiation patterns of the designed DRAA (solid lines), measurements of the prototype from [12] (dash-dot lines) and simulated radiation patterns of the equivalent monofocal antenna (dotted lines).

In some applications, as in the case of multi-beam satellite antennas that provide a multi-spot coverage in Ka-band [14]-[17] the bifocal technique can be used to obtain a reduced separation between adjacent beams. This requirement normally leads to offset DRAA configurations with a convex phase curve on the sub-reflectarray and a concave one on the main reflectarray, as can be observed in Fig. 3 (dashed lines) when the beam directions in the previous bifocal design (associated to feeds 2 and 6) are changed to $\theta_{b1/2} = \pm 5$º (for 2.5º beam spacing). Note that the samples obtained after the ray tracing are very close on the sub-reflectarray and present a larger spacing on the main reflectarray, which yields a smaller sub-reflector for the same main reflectarray size. These results are suitable to avoid blockage in offset configurations.

IV. DESIGN OF A MULTI-BEAM DUAL REFLECTARRAY ANTENNA IN KA-BAND

The bifocal technique has been used to design a multi-beam DRAA to provide 0.56º of beam spacing at 20 GHz for broadband satellite communications in Ka-band, considering 54-mm diameter feeds for the illumination [14]. The initial parameters of the DRAA system are: d = 27.5 cm, L_1 = 1.3 m, L_2 = 2.42 m, θ_{b1} = 1.4º and θ_{b2} = -1.4º. An offset configuration has been formed by a 60-cm sub-reflectarray and a 180-cm main reflectarray, whose geometrical centers are located at C_S = (0.4, 2.42, 0) m and C_M = (1.7, 0, 0) m. The phase distributions obtained with the reflectarrays in parallel planes (given in Fig. 5(a) and 5(b)) present a large number of phase cycles, especially in the case of the main reflectarray. The tilt angles applied to each reflectarray to obtain a smoother phase variation are θ_S = 8º and θ_M = 13.5º. Figures 5(c) and 5(d) show the phase distributions obtained for the tilted DRAA (given in Fig. 6) after applying the required phase adjustment. The simulated radiation patterns (assuming ideal reflectarray cells) of the DRAA before and after tilting the reflectarrays are very similar, as shown in Fig. 7. The effective aperture of the antenna is reduced due to the main reflectarray tilt, which causes a small loss in gain (-1.3 dB). The aperture efficiency of the DRAA is around 40%, although this value can be improved if the bifocal technique is applied to obtain a larger beam spacing, e. g., the design of a multi-beam DRAA for 1.12º beam spacing achieves around 60-65% efficiency at 20 GHz, as shown in [22].

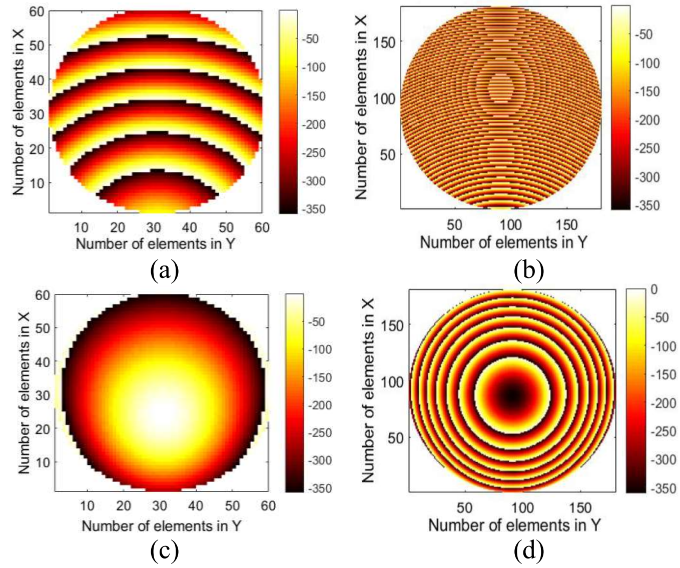

Fig. 5 Required bifocal phase distributions (deg.) at 20 GHz before tilting (a) on the sub-reflectarray and (b) the main reflectarray, and after tilting (c) on the sub-reflectarray and (d) the main reflectarray.

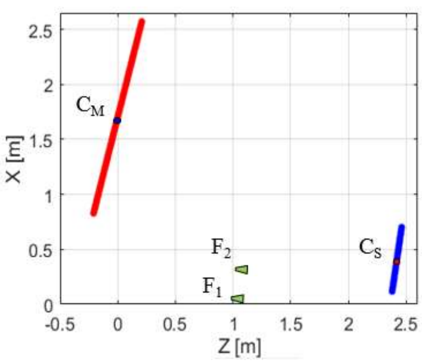

Fig. 6 Geometry of the tilted dual reflectarray antenna.

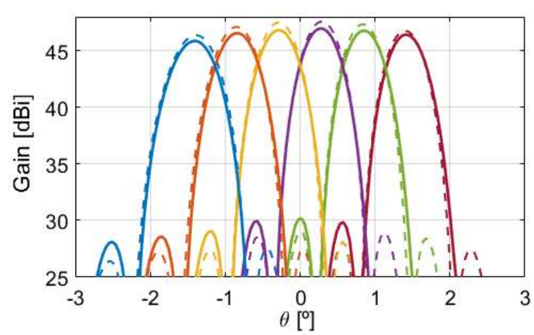

Fig. 7 Simulated radiation patterns at 20 GHz for the multi-beam DRAA before (dashed lines) and after (solid lines) tilting the reflectarrays.

V. CONCLUSION

A novel bifocal procedure has been proposed for the design of dual reflectarray antennas in offset configurations, starting from a symmetric geometry with parallel reflectarrays. The technique has been validated by comparison with a folded DRAA prototype. Then, a multi-beam DRAA in Ka-band with 0.56º beam spacing has been designed. The radiation patterns for the DRAA with tilted reflectarrays are in good agreement with those obtained for the axially symmetric configuration.

REFERENCES

[1] B. L. Rao, "Bifocal dual reflector antenna", *IEEE Trans. Antennas Propag*., vol. 22, no. 9, pp. 711-714, Sept. 1974.

[2] M. E. Lorenzo, C. M. Rappaport, and A. G. Pino, "A bifocal reflector antenna with Gregorian configuration", in *Proc. IEEE Antennas Propag. Soc. Int. Symp. (APSURSI)*, vol. 1, Jul. 1996, pp. 234-237.

[3] A. Garcia-Pino, N. Llombart, B. Gonzalez-Valdes and O. Rubiños-López, "A bifocal ellipsoidal Gregorian reflector system for THz imaging applications", *IEEE Trans. Antennas Propag*., vol. 60, no. 9, pp. 4119-4129, Sept. 2012.

[4] A. Garcia-Pino, B. Gonzalez-Valdes, O. Rubiños, J. Grajal, A. Badolato, B. Mencia-Oliva, Pilar García Soidán and J. L. Besada-Sanmartín, "Bifocal reflector antenna for a standoff radar imaging system with enhanced field of view", *IEEE Trans. Antennas Propag*., vol. 62, no. 10, pp. 4997-5006, Oct. 2014.

[5] C. M. Rappaport, "An offset bifocal reflector antenna design for wide-angle beam scanning", *IEEE Trans. Antennas Propag*., vol. 32, no. 11, pp. 1196-1204, Nov. 1984.

[6] A. N. Plastikov, "A high-gain multibeam bifocal reflector antenna with 40º field of view for satellite ground station applications", *IEEE Trans. Antennas Propag*., vol. 64, no. 7, pp. 3251-3254, Jul. 2016.

[7] D. Zhou, L. Hou, M. Pan, "Bifocal Gregorian reflector antenna designed for terahertz imaging", *10th UK-Europe-China Workshop on Millimetre Waves and Terahertz Technologies (UCMMT)*, Sept. 2017.

[8] C. Tienda, M. Arrebola, J. A. Encinar, and G. Toso, "Analysis of a dual-reflectarray antenna," *IET Microw. Antennas Propag*., vol. 5, no. 13, pp. 1636–1645, Oct. 2011.

[9] C. Tienda, J. A. Encinar, M. Arrebola, M. Barba and E. Carrasco, "Design manufacturing and test of a dual-reflectarray antenna with improved bandwidth and reduced cross-polarization", *IEEE Trans. Antennas Propag*., vol. 61, no. 3, pp. 1180-1190, March 2013.

[10] S. Montori, F. Cacciamani, R. V. Gatti, R. Sorrentino, G. Arista, C. Tienda, J. A. Encinar and G. Toso, "A transportable reflectarray antenna for satellite Ku-band emergency communications", *IEEE Trans. Antennas Propag*., vol. 63, no. 4, pp. 1393-1407, Apr. 2015.

[11] J. Zhao, T. Li, X. Cui, X. Zhao, H. Li, B. Hu, H. Wang, Y. Zhou, Q. Liu, "A low-mutual coupling dual-band dual-reflectarray antenna with the potentiality of arbitrary polarizations", *IEEE Antennas Wireless Propag. Lett.*, vol. 16, pp. 3224-3227, Nov. 2017.

[12] W. Menzel, M. Al-Tikriti and R. Leberer, "A 76-GHz multiple-beam planar reflector antenna", in *Proc. 32nd Eur. Microw. Conf*., Milan, Italy, Sept. 2002.

[13] J. G. Cuevas, C. Tienda, J. A. Encinar and G. Krieger, "Principle of bifocal antennas implemented in a dual reflectarray configuration", in *Proc. 9th Eur. Conf. Antennas Propag. (EuCAP)*, Lisbon, Portugal, April 2015.

[14] M. Schneider, C. Hartwanger and H. Wolf, "Antennas for multiple spot beams satellites", *CEAS Space Journal*, vol. 2, pp. 59-66, Dec. 2011.

[15] H. Fenech, S. Amos, A. Tomatis and V. Soumpholphakdy, "High throughput satellite systems: An analytical approach," in *IEEE Trans. Aerosp. Electron. Syst.*, vol. 51, no. 1, pp. 192-202, Jan. 2015.

[16] B. Palacin, N. J. G. Fonseca, M. Romier, R. Contreres, J. C. Angevain, G. Toso and C. Mangenot, "Multibeam antennas for very high throughput satellites in Europe: Technologies and trends", in *Proc. 11th Eur. Conf. Antennas Propag. (EuCAP)*, Paris, France, April 2017, pp. 2413-2417.

[17] M. Zhou and S. B. Sørensen, "Multi-spot beam reflectarrays for satellite telecommunication applications in Ka-band," in *Proc. 10th Eur. Conf. Antennas Propag., (EuCAP),* Davos, Switzerland, Apr. 2016.

[18] J. Rodriguez-Alvarez, M. Arrebola, C. Tienda, J. A. Encinar, and F. Las-Heras, "Bifocal antenna based on dual-reflectarray dual-offset configuration," in *Proc. 6th Eur. Conf. Antennas Propag. (EuCAP)*, Prague, Czech Republic, Mar. 2012, pp. 2348–2352.

[19] E. Martinez-de-Rioja, J. A. Encinar, A. Pino, B. Gonzalez-Valdes, C. Tienda, S. V. Hum and G. Toso, "Application of bifocal concept to dual reflectarray configurations for multi-beam satellite antennas in Ka-band", in *Proc. 11th Eur. Conf. Antennas Propag. (EuCAP)*, Paris, France, March 2017, pp. 2427-2430.

[20] R. Florencio, J. A. Encinar, R. R. Boix, V. Losada and G. Toso, "Reflectarray antennas for dual polarization and broadband Telecom satellite applications", *IEEE Trans. Antennas Propag*., vol. 63, no. 4, pp. 1234-1246, Apr. 2015.

[21] M. Hosseini and S. V. Hum, "A dual-CP reflectarray unit cell for realizing independently controlled beams for space applications", in *Proc. 11th Eur. Conf. Antennas Propag.(EuCAP)*, Paris, France, April 2017, pp. 66-70.

[22] E. Martinez-de-Rioja, J. A. Encinar, C. Geaney, S. V. Hum, and A. Pino, "Study of Bifocal Dual Reflectarray Configurations for Multi-Beam Antennas in Ka-band", in *Proc. IEEE Antennas Propag. Soc. Int. Symp. (APSURSI)*, San Diego, California, USA, July 2017, pp. 1183-1184.